



HAL
open science

Thermal Expansion of Magnetite (4.2 - 300 K)

Yvette Hancock, Trevor Roy Finlayson

► **To cite this version:**

Yvette Hancock, Trevor Roy Finlayson. Thermal Expansion of Magnetite (4.2 - 300 K). *Philosophical Magazine*, 2009, 89 (22-24), pp.1913-1921. 10.1080/14786430802647057 . hal-00514007

HAL Id: hal-00514007

<https://hal.science/hal-00514007>

Submitted on 1 Sep 2010

HAL is a multi-disciplinary open access archive for the deposit and dissemination of scientific research documents, whether they are published or not. The documents may come from teaching and research institutions in France or abroad, or from public or private research centers.

L'archive ouverte pluridisciplinaire **HAL**, est destinée au dépôt et à la diffusion de documents scientifiques de niveau recherche, publiés ou non, émanant des établissements d'enseignement et de recherche français ou étrangers, des laboratoires publics ou privés.



Thermal Expansion of Magnetite (4.2 – 300 K)

Journal:	<i>Philosophical Magazine & Philosophical Magazine Letters</i>
Manuscript ID:	TPHM-08-Oct-0372
Journal Selection:	Philosophical Magazine
Date Submitted by the Author:	16-Oct-2008
Complete List of Authors:	Hancock, Yvette; Department of Engineering Physics, Helsinki University of Technology, PO Box 4100, FI-02015 HUT, FINLAND Finlayson, Trevor; School of Physics, University of Melbourne, Victoria 3010, AUSTRALIA
Keywords:	magnetism, thermal expansion
Keywords (user supplied):	magnetite, three-terminal capacitance dilatometry, Verwey transition
<p>Note: The following files were submitted by the author for peer review, but cannot be converted to PDF. You must view these files (e.g. movies) online.</p>	
<p>Hancock_submit.tex</p>	



Philosophical Magazine
Vol. 00, No. 00, 2008, 1–8

RESEARCH ARTICLE

Thermal Expansion of Magnetite (4.2 – 300 K)

Y. Hancock^{a*} and T.R. Finlayson^b

^a*Department of Engineering Physics, Helsinki University of Technology, PO Box 4100, FI-02015 HUT, Finland;* ^b*School of Physics, University of Melbourne, Victoria 3010, Australia*

(Received 00 Month 200x; final version received 00 Month 200x)

The thermal expansion of a synthetic single crystal sample of magnetite (Fe_3O_4) in the [111] direction has been investigated for the temperature range of 4.2 – 300 K using three-terminal capacitance dilatometry. The strain results and corresponding thermal expansion curve show the Verwey transition to be first-order with $T_v = 120 \pm 2$ K. At $T = 4.2 - 70$ K, the sample shows Invar-like behaviour.

Keywords: magnetite; Verwey transition; three-terminal capacitance dilatometry; thermal expansion

1. Introduction

Magnetite (Fe_3O_4), or common lodestone, is the oldest known magnetic material, having been discovered by the ancient Greeks around 1500 B.C. [1]. Magnetite has had a long research history—before the 19th century it was the only material known to be a permanent magnet at room temperature. An important property of magnetite is the Verwey transition, which is a first-order metal insulator transition resulting from a slight distortion in the crystal structure from inverse cubic spinel to monoclinic, and occurring at $T_v \sim 120$ K [2–4]. The Verwey transition manifests itself as a decrease in the electrical conductivity [5], magnetization [6] and thermal expansion [7], together with a peak in the specific heat [8] at the transition point. Despite intense research efforts, there is still a lot of controversy surrounding the microscopic mechanism of this transition in magnetite, as well as the specific structure of this system below the transition temperature [9–14].

Little has been reported on the low temperature thermal expansion properties of magnetite, which is one means of characterising the Verwey transition. In this work, we contribute to the understanding of this property by showing the thermal expansion of a synthetic single crystal sample, which has been measured using three-terminal capacitance dilatometry at a temperature range of 4.2 – 300 K. A complete description of the three-terminal capacitance dilatometry method has been reported elsewhere [15, 16]. The technique is highly accurate and capable of measuring small changes in sample length l_s to within $\delta l_s = \pm(0.5 - 50)$ Å.

A survey of the literature reveals that the reported thermal expansion results of magnetite have a lower level of accuracy, poorer sample purity, or cover a small

*Corresponding author. Email: yvh@fyslab.hut.fi

temperature range. A similar dilatometric technique used by Domenicali [17], for example, erroneously reports on the transition being of second order with T_v measured at ~ 109 K via the thermal expansion of a natural single crystal sample. In other work, Bickford, who uses a strain gauge to measure the thermal expansion of a synthetic single crystal sample, reports on a first order Verwey transition at 118 K with a strain error of $\sim 10^{-6}$ [7]. Both measurements occur over a short temperature range between 90 – 130 K. In comparison, our results show the thermal expansion of a high purity synthetic sample obtained by three-terminal capacitance dilatometry, which correctly demonstrates a first-order transition at $T_v \sim 120$ K and covers an extensive temperature range of 4.2 – 300 K. At low temperatures (4.2 – 70 K), our results also show that magnetite exhibits Invar-like behaviour [18], which to our knowledge has not been reported on for a single crystal sample.

2. Experimental Method

2.1. Thermal Expansion and Three Terminal Capacitance Dilatometry

The linear thermal expansion coefficient, α , is defined as the fractional change in length of a sample, $\Delta l_s/l_{s0}$, or strain, per degree temperature change, $\Delta T(K)$, such that,

$$\alpha = \frac{1}{l_{s0}} \frac{\Delta l_s}{\Delta T}, \quad (1)$$

where l_{s0} denotes the initial length of the sample. Such measurements can be made using three-terminal capacitance dilatometry. A full description of the dilatometry method has already been described in the literature [15, 16], thus only a brief explanation is given here.

Figure 1 (left) shows a schematic diagram of the thermal expansion cell and cryostat used in these experiments [15]. In Figure 1 (right), the relevant cell parameters are indicated [16]. Small changes in the sample length Δl_s can be determined by measuring changes in the capacitance gap Δg . The relationship between the capacitance C and the cell geometric parameters is given by White [19], where,

$$C = \frac{\pi r^2}{g} \left(1 + \left(\frac{w}{r} \right) \frac{1 + \frac{w}{2r}}{1 + 0.22 \frac{w}{g}} \right). \quad (2)$$

Here, r is the radius of the top plate and w is the width of the guard ring (Figure 1). A typical gap width of $g = 0.2$ mm together with room temperature values for r and w at $T = 293$ K are used to approximate the above expression [16]. Hence,

$$g = \frac{k}{C}, \quad (3)$$

where k is a constant. The change in sample length Δl_s over a temperature difference ΔT is determined from the measured capacitance and calculated gap in Equation (3), such that,

$$\Delta g = \Delta l_{cell} = \Delta l_s + \Delta l_{Cu}, \quad (4)$$

where Δl_{Cu} refers to the temperature dependence of the length of the two copper plates between which the sample sits. From Equation (1), the linear thermal expansion co-efficient, α , is then determined at temperature increments of ΔT .

2.2. *Synthetic Single Crystal Specimen and Thermal Expansion Measurements*

The single crystal specimen of magnetite was made at the University of Minnesota [20]. The impurities and relative concentrations found in this specimen were obtained by spectroscopic analysis and are shown in Table 1. The sample was reported to have a total impurity concentration of 1.14%. The purity of the sample is considered to be better than this, however, as the major impurity element, silicon (Si) was thought to be present in bits of quartz and calcite on the specimen surface [20].

The sample was visually inspected using an optical microscope and was found to be octahedral in shape, consisting of eight natural triangular facets. The minimisation of tilt is an important factor for reducing errors in the thermal expansion measurements, therefore the parallelism of each of the four opposing pairs of faces of the specimen was measured using an optical autocollimator. The pair of faces selected from the sample were those with the smallest tilt, which was measured as 5.3 ± 0.5 minutes of arc. The dimension of the sample was determined from the distance between the selected opposite facet faces. This was measured as 2.343 ± 0.005 mm using a micrometer.

The orientation of the crystal was established using Laue back-reflection. The sample was mounted onto a two-axis goniometer and irradiated using X-rays from a cobalt tube operating at 350 W, with an accelerating voltage of 36 kV and current of 8 mA. From the X-ray images, the symmetry of the pattern was determined as being three-fold, which for a cubic crystal implies that the direction normal to the X-ray beam is [111]. The experimental results were found to compare favourably with the standard Laue back-reflection pattern for a single crystal orientated in that direction.

The total length of the thermal expansion cell, l_{cell} , was fixed at 50.824 ± 0.005 mm (Figure 1). In order to obtain a gap of 0.2 mm, a copper spacer of $\simeq 43.214 \pm 0.005$ mm in length was made out of oxygen free, high conductivity, high purity copper. The three springs required to hold the sample and copper pieces together provided a force of 2.6 N. Once the specimen had been assembled, the total tilt was measured for the sample assembly using an optical autocollimator, which was again determined to be 5.3 ± 0.5 minutes of arc. The sample assembly was then placed inside of the thermal expansion cell (Figure 1).

Two heating runs were performed, which consisted of a liquid nitrogen run ($T = 77 - 300$ K) and a liquid helium run ($T = 4.2 - 77$ K). A liquid nitrogen cooling run was also performed ($T = 135 - 77$ K), which was required for testing thermal hysteresis in the sample. For the liquid nitrogen heating run, the cell was initially cooled to 77 K. This was done by filling both the outer and inner dewars of the cryostat with liquid nitrogen. Several shots of helium exchange gas were injected into the outer vacuum chamber (OVC), which was required to quickly reduce the temperature of the cell. Once the equilibrium temperature had been attained, the OVC was then evacuated until a pressure of $< 10^{-6}$ Torr was reached to thermally

1 insulate the capacitance cell. This pressure was then maintained throughout the
2 experiment. Temperatures above 77 K were obtained by using a heating element
3 around the top of the cell. The temperature of the cell was varied by passing a small
4 current through the coil, sufficient to increase the temperature by small increments.
5

6 To obtain results for temperatures between 4.2 and 77 K, liquid helium was
7 used as the inner dewar coolant. Temperature cycles were performed for expansion
8 measurements below 35 K (Figure 2). These cycles were necessary to correct for
9 the effects of electronic drift and cell hysteresis by regularly recooling the sample
10 to 4.2 K.

11 The capacitance was measured when thermal equilibrium in the chamber had
12 been achieved by balancing a *GR1616 Precision Capacitance Bridge*, which is ca-
13 pable of 0.1 aF resolution for measured capacitances up to 11 pF [16]. The tem-
14 perature of the cell was then measured using two types of thermometer. From 2
15 – 22 K, a calibrated germanium cryoresistor was used, and a calibrated four-wire
16 platinum resistor used for temperatures between 22 and 300 K (Figure 1). At least
17 one hour between measurements was required to ensure temperature stabilisation.
18

19 For all temperature runs, the calculation of α (Equation 1) was made from two
20 capacitance readings taken ΔT apart, where the value of α was defined at the
21 midpoint of ΔT . These pairs of readings from which the α values were obtained
22 were themselves spaced at various temperature intervals depending on the type of
23 run used.
24
25
26
27

28 3. Results and Discussion

29
30 The strain vs. temperature curve for the [111] direction of the synthetic Fe_3O_4 sin-
31 gle crystal sample (Figure 3) was determined from the capacitance measurements
32 (Equations 2–4). For $T < 100$ K, the error in capacitance, δC , of $\pm (2 - 5)$ aF, cor-
33 responds to an error in sample length, $\delta l = (0.5 - 2)$ Å. For temperatures between
34 100 and 300 K, $\delta C = \pm (50 - 100)$ aF and $\delta l = (10 - 50)$ Å [21]. Larger errors
35 occur for $T > 77$ due to thermal fluctuations in the capacitance cell. Errors caused
36 by the tilt of the capacitance plates, and hence from a non-ideal capacitance gap,
37 were also taken into account. The temperature ranges and their associated errors
38 in the strain, $\delta(\Delta l_s/l_{s0})$ are given in Table 2, with corresponding error bars in
39 Figure 3. The strain results are a derived quantity, therefore the main source of
40 error in this value (Table 2) is in the micrometer measurement of the very small
41 sample length, which was of order $\delta l_{s0} \sim 10^{-6}$ m.

42
43 Figure 3 shows a discrete jump in the strain results, which corresponds to the
44 Verwey transition at $T_v = (120 \pm 2)$ K. The uncertainty in T_v was determined
45 from the temperature range over which the transition occurs, together with the
46 uncertainty in the temperature reading—for both thermometers this was estimated
47 as ± 0.05 K [16]. The anomalous jump that appears in the strain results at ~ 77 K
48 (Figure 3) is due to thermal instability in the cell upon changing the coolant from
49 liquid helium to liquid nitrogen.
50

51 The percentage change in strain in the sample going through the Verwey transi-
52 tion (Figure 3) was determined as $\sim 0.009\%$, compared with $\sim 0.06\%$ for Bickford's
53 synthetic single crystal sample [7]. The difference in percentage strain between
54 these two measurements can be explained by the highly anisotropic nature of the
55 thermal expansion in magnetite [7]. Thus, a slight misalignment of the sample
56 would amount to a significant change in the thermal expansion measurement at
57 the transition, hence explaining the large discrepancy in the results.
58

59 The thermal expansion results for the single crystal sample (Figure 4) are derived
60

1 from the strain results (Figure 3) using Equation 1. The temperature ranges and
2 their associated errors in the thermal expansion coefficient, $\delta\alpha$, for the magnetite
3 single crystal, are given in Table 2. The errors in $\delta\alpha$ are derived from the errors
4 in the strain results and temperature readings, in accordance with Equation 1.
5 The Verwey transition point, T_v , is clearly defined, showing a sharp peak in the
6 variation of the expansion coefficient with temperature (Figure 4). Results from
7 both temperature increasing (circles) and temperature decreasing (stars) runs are
8 shown and a small thermal hysteresis at T_v is observed. For temperatures below
9 T_v , the expansion coefficient is extremely small and for the temperature range
10 $4.2 < T < 70$ K (as shown in the insert to Figure 4) it is less than 1.2×10^{-6}
11 K^{-1} , reminiscent of the small expansion coefficient known for the Fe-36at%Ni alloy
12 (Invar) [22]. In the case of the Invar alloy, the unusually small expansion coefficient
13 arises from a balance between a negative, magnetovolume contribution arising from
14 energetically unsatisfied Fe-Fe bonds (magnetic frustration) [23] and the normal
15 anharmonic lattice expansion.
16

17
18 The Invar-like behaviour has, to our knowledge, not been previously reported for
19 single-crystal magnetite. While the present result has only been recorded for the
20 [111] direction of our single-crystal sample, it is worth noting that for a sample
21 of polycrystalline, natural magnetite, which was also measured during the same
22 project, the thermal expansion coefficient was less than $0.4 \times 10^{-6} \text{K}^{-1}$ at $4.2 < T$
23 < 70 K. A similar value of α for a natural magnetite sample was also found in the
24 literature [24]. For the previously reported thermal expansion data for a synthetic
25 single crystal of magnetite [7], the author did not extend the measurements to
26 temperatures that were very far below the Verwey transition temperature.
27

28 It is well documented that the Verwey transition is sensitive to impurity content,
29 internal stress and other types of structural imperfections [9]. Therefore, the sharp-
30 ness of the peak in the thermal expansion coefficient at T_v (Figure 4) and the value
31 of T_v indicate that the sample is of high purity. The discontinuity in the strain and
32 thermal hysteresis at the transition are consistent with it being a first-order tran-
33 sition, which has also been previously illustrated from measurements that show an
34 accompanying volume change [7].
35

36 37 38 4. Conclusions

39
40 Three-terminal capacitance dilatometry was used to measure the strain and to de-
41 termine the thermal expansion of a high-purity synthetic single crystal of magnetite
42 in the [111] direction. Both heating and cooling runs were performed over a tem-
43 perature range of 4.2 – 300 K. The results show a well defined Verwey transition
44 with thermal hysteresis at $T_v = 120 \pm 2$ K, which corresponds to a discontinuity
45 in strain ($\sim 0.009\%$) in the sample, and a sharp peak in the thermal expansion co-
46 efficient. These results are consistent with the Verwey transition being a first-order
47 transition. For temperatures below T_v , the crystal exhibits Invar-like expansion
48 behaviour.
49

50 51 52 5. Acknowledgements

53
54 We should like to thank Dr. Andrew Prentice (Monash University) for his original
55 request for a number for the low-temperature expansion coefficient for magnetite,
56 which gave rise to this project, and to acknowledge Dr. Henry Pinto (HUT) and
57 Dr. Guy White (formerly of CSIRO) for helpful discussions.
58
59
60

References

- [1] Z. Zhang and S. Satpathy, Phys. Rev. B 44 (1991) p.13319.
- [2] E.J.W. Verwey, Nature (London) 144 (1939) p.327.
- [3] M. Iizumi, T.F. Koetzle, G. Shirane, *et al.*, Acta Crystallogr. B 38 (1982) p.2121.
- [4] J.P. Wright, J.P. Attfield and P.G. Radaelli, Phys. Rev. Lett. 87 (2001) p.266401.
- [5] S. Iida, Phil. Mag. B 42 (1980) p.349.
- [6] P. Weiss and R. Forrer, Ann. Phys. 12 (1929) p.279.
- [7] L.R. Bickford, Rev. Mod. Phys. 25 (1953) p.75.
- [8] R.W. Millar, J. Amer. Chem. Soc. 51 (1929) p.215.
- [9] F. Walz, J. Phys.: Condens. Matter 14 (2002) p.R285.
- [10] M. Coey, Nature 430 (2004) p.155.
- [11] J. García and G. Subís, J. Phys.: Condens. Matter 16 (2004) p.R145.
- [12] E. Nazarenko, J.E. Lorenzo, Y. Joly *et al.*, Phys. Rev. Lett. 97 (2006) p.056403.
- [13] I. Leonow, A.N. Yaresko, V.N. Antonov *et al.*, Phys. Rev. Lett. 93 (2004) p.146404.
- [14] H.P. Pinto and S.D. Elliott, J. Phys.: Condens. Matter 18 (2006) p.10427.
- [15] G.K. White and J.G. Collins, Journal of Low Temperature Physics 7 (1972) p.43.
- [16] E.E. Gibbs, PhD thesis, Monash University, Australia (1983).
- [17] C.A. Domenicali, Phys. Rev. 78 (1950) p.458.
- [18] C.E. Guillaume, C. R. Acad. Sci. 125 (1897) p.235.
- [19] G.K. White, Cryogenics 1 (1961) p.151.
- [20] D.B. Bonstrom, PhD thesis, University of Minnesota, Minnesota, USA (1959).
- [21] M. Liu, PhD thesis, Monash University, Australia (1991).
- [22] <http://en.wikipedia.org/wiki/Invar>
- [23] D.G. Rancourt and M.-Z. Dong, Phys. Rev. B 54 (1996) p.12225.
- [24] E.Y. Aksenova, V.N. Gorbach and Y.A. Mamalui, Sov. Phys. Solid State 29 (1987) p.490.

Peer Review Only

Table 1. Impurities and percentage concentrations for the synthetic single crystal magnetite sample. The concentrations were obtained using spectroscopic analysis and were determined from the relative line intensities [20].

Cation	% Concentration
Si	1.0
Ca	0.1
Cr	none detected
Ba	none detected
Ti	0.01
Mg	0.01
V	0.001
Cd	0.01
Co	0.001
Ni	0.001
Cu	0.01

Table 2. Calculated errors in the strain $\delta(\Delta l_s/l_{s0})$ and linear thermal expansion co-efficient $\delta\alpha$ (K^{-1}) measurements as a function of the temperature range.

T (K)	$\delta(\Delta l_s/l_{s0})$	$\delta\alpha$ (K^{-1})
4.2 – 25	7×10^{-6}	4×10^{-7}
25 – 77	1×10^{-5}	1×10^{-6}
> 77	2×10^{-5}	2×10^{-6}

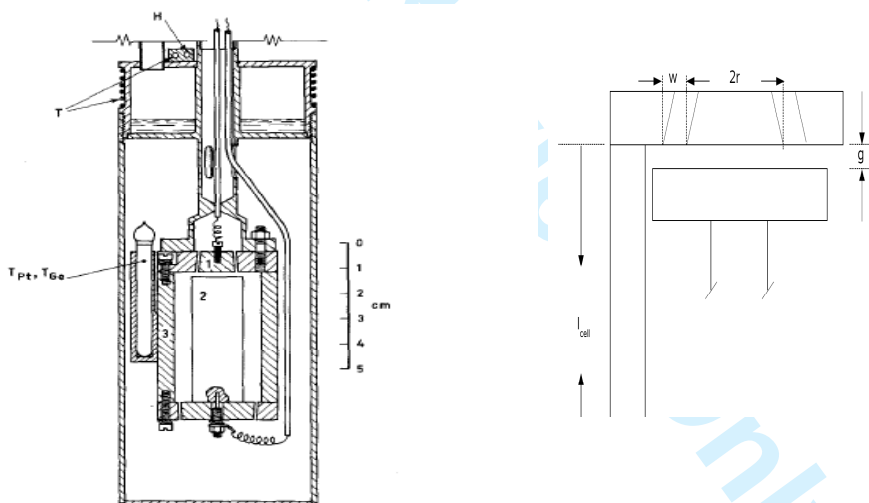


Figure 1. (Left) Diagram showing the inner vacuum chamber of the three-terminal capacitance dilatometer (reproduced from White and Collins [15]). T_{Pt} and T_{Ge} refer to the platinum and germanium thermometers, respectively. Section 1 = copper top plate, 2 = sample assembly unit, and 3 = the copper casing of the thermal expansion cell. (Right) Schematic showing the essential parameters of the thermal expansion cell. Here, g is the capacitance gap, l_{cell} is the total cell length, w is the width of the guard ring, and r is the radius of the top plate.

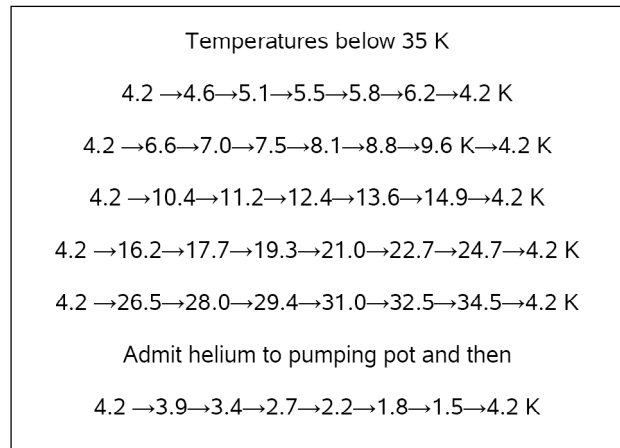


Figure 2. Temperature cycles for thermal expansion measurements below 35 K.

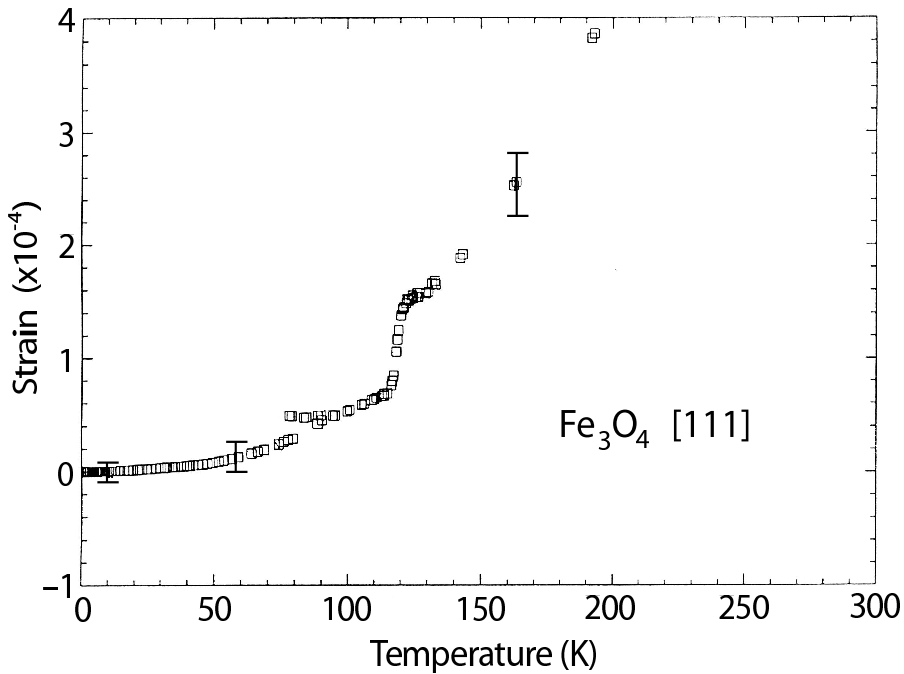


Figure 3. Graph of strain vs. temperature in the [111] direction for the synthetic single crystal magnetite sample ($T = 4.2 - 300$ K). The Verwey transition is indicated by the discontinuity in the strain at $T_v = 120 \pm 2$ K. The anomalous jump in the strain results at 77 K corresponds to the thermal instability in the capacitance cell due to the change in coolant from liquid Helium to liquid Nitrogen.

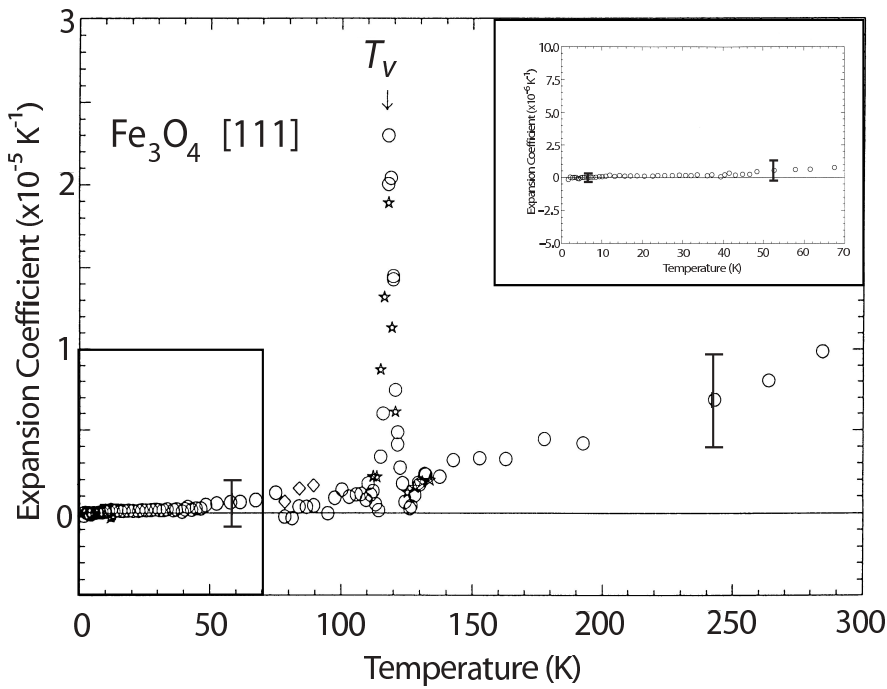
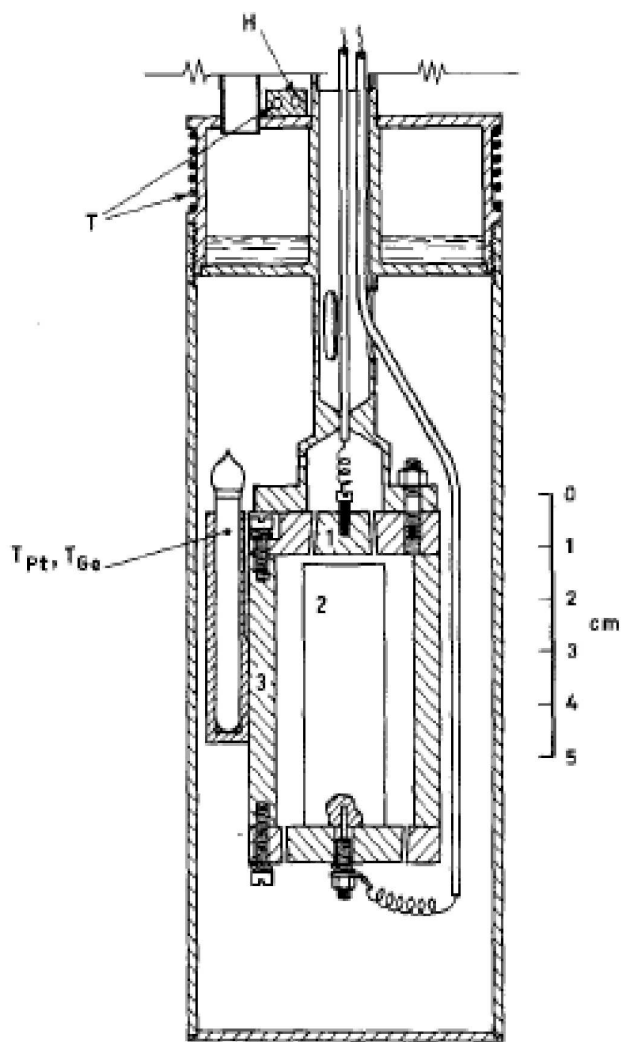


Figure 4. Graph of the linear thermal expansion co-efficient (α) vs. temperature for the synthetic single crystal magnetite sample in the [111] direction ($T = 4.2 - 300 \text{ K}$). Circles refer to the heating run and stars refer to the cooling run. The Verwey transition is indicated by the sharp peak in the expansion co-efficient. The insert shows the Invar-like behaviour of the sample at $4.2 - 70 \text{ K}$.

Review Only

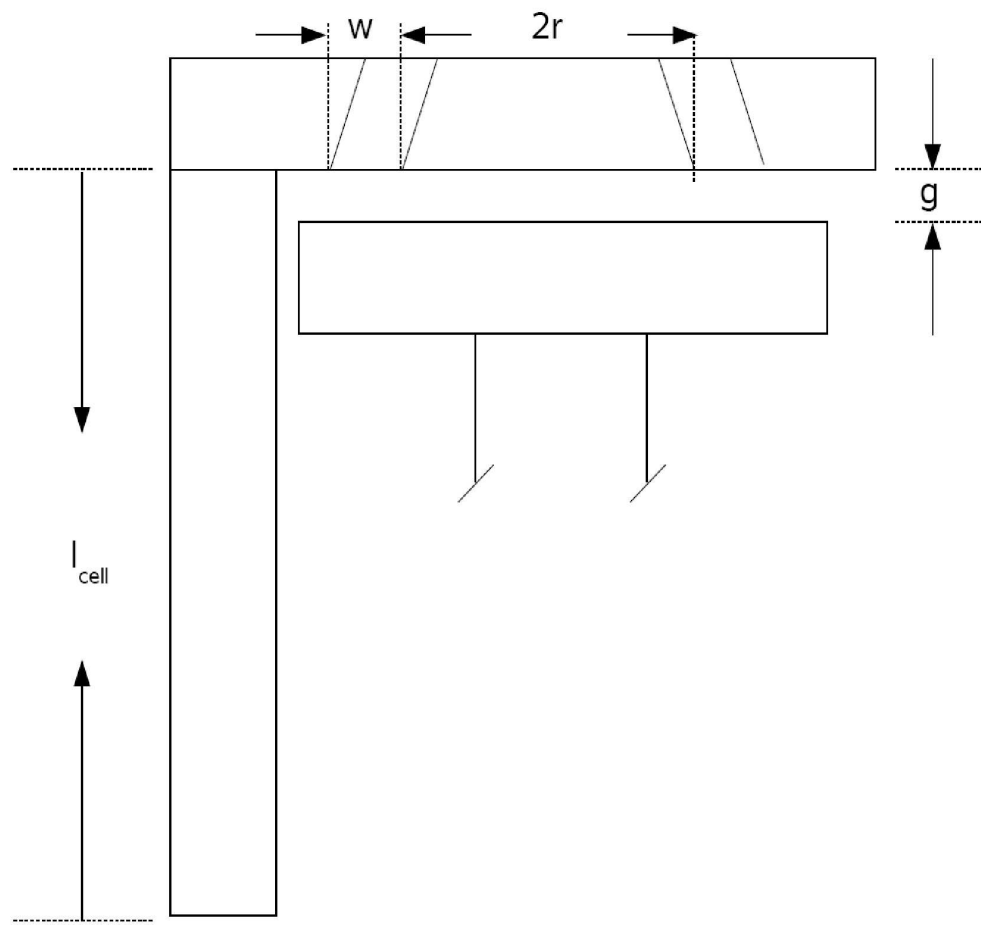
1
2
3
4
5
6
7
8
9
10
11
12
13
14
15
16
17
18
19
20
21
22
23
24
25
26
27
28
29
30
31
32
33
34
35
36
37
38
39
40
41
42
43
44
45
46
47
48
49
50
51
52
53
54
55
56
57
58
59
60



141x152mm (600 x 600 DPI)



1
2
3
4
5
6
7
8
9
10
11
12
13
14
15
16
17
18
19
20
21
22
23
24
25
26
27
28
29
30
31
32
33
34
35
36
37
38
39
40
41
42
43
44
45
46
47
48
49
50
51
52
53
54
55
56
57
58
59
60



360x379mm (600 x 600 DPI)



Temperatures below 35 K

4.2 → 4.6 → 5.1 → 5.5 → 5.8 → 6.2 → 4.2 K

4.2 → 6.6 → 7.0 → 7.5 → 8.1 → 8.8 → 9.6 K → 4.2 K

4.2 → 10.4 → 11.2 → 12.4 → 13.6 → 14.9 → 4.2 K

4.2 → 16.2 → 17.7 → 19.3 → 21.0 → 22.7 → 24.7 → 4.2 K

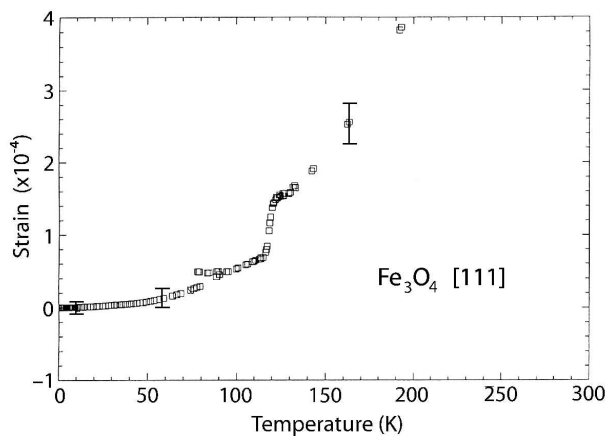
4.2 → 26.5 → 28.0 → 29.4 → 31.0 → 32.5 → 34.5 → 4.2 K

Admit helium to pumping pot and then

4.2 → 3.9 → 3.4 → 2.7 → 2.2 → 1.8 → 1.5 → 4.2 K

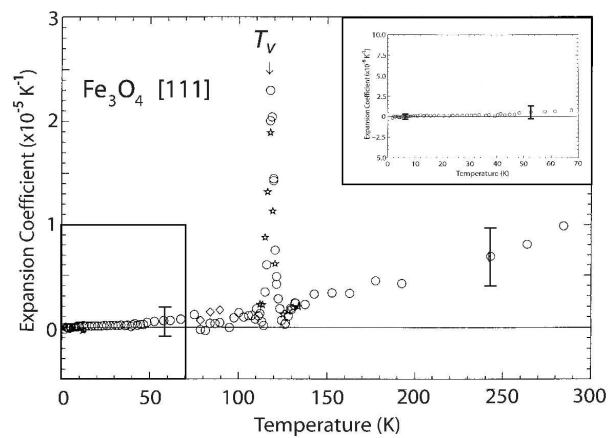
378x299mm (600 x 600 DPI)

1
2
3
4
5
6
7
8
9
10
11
12
13
14
15
16
17
18
19
20
21
22
23
24
25
26
27
28
29
30
31
32
33
34
35
36
37
38
39
40
41
42
43
44
45
46
47
48
49
50
51
52
53
54
55
56
57
58
59
60



209x297mm (600 x 600 DPI)

1
2
3
4
5
6
7
8
9
10
11
12
13
14
15
16
17
18
19
20
21
22
23
24
25
26
27
28
29
30
31
32
33
34
35
36
37
38
39
40
41
42
43
44
45
46
47
48
49
50
51
52
53
54
55
56
57
58
59
60



209x297mm (600 x 600 DPI)